# LANGMUIR

pubs.acs.org/Langmuir Article

# Ionic Liquid Solutions Show Anomalous Crowding Behavior at an Electrode Surface

Travis Douglas, Sangjun Yoo, and Pulak Dutta\*



Cite This: https://doi.org/10.1021/acs.langmuir.2c00036



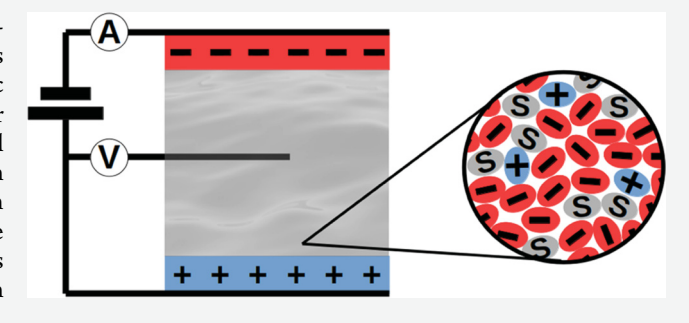
**ACCESS** I

Metrics & More



Supporting Information

**ABSTRACT:** X-ray reflectivity was used to study the several-nanometer-thick "crowded" layers that form at the interfaces between a planar electrode and concentrated solutions of ionic liquids. The ionic liquid  $[P_{14,6,6,6}]^+[NTf_2]^-$  was dissolved in either strongly polar propylene carbonate or weakly polar dimethyl carbonate. In the range of 19–100 vol % ionic liquid, between working electrode potentials +2 and +2.75 V, uniform 2–7 nm thick interfacial layers were observed. These layers are not pure anions but contain three to five times as many anions as cations and about the same percentage of solvent as the bulk solution. On the other side of the layer, the density is that of the bulk solution.



These features are inconsistent with a picture of the crowded layer as a region of pure, close-packed counterions. Not only the layer thickness but also the charge density decrease with increasing dilution at any given applied voltage. This appears to indicate, counterintuitively, that a thinner layer with lower net charge density will screen an electric field as effectively as a thicker layer with higher charge density.

#### ■ INTRODUCTION

As there is a growing demand for energy, the need for more advanced energy storage devices becomes apparent. Recently, ionic liquids (ILs) have received much attention as alternative electrolytes with novel properties that may prove useful for energy storage. Room-temperature ILs (RTILs) are salts that are liquid even at room temperature due to the weak bonding between the cation and anion. Pure ionic liquids are composed entirely of charged cations and anions, a system far removed from the dilute electrolyte case, where ions may reasonably be considered to behave as noninteracting point charges and the solvent as a dielectric continuum.<sup>2</sup> The high concentration of ions interacting via the long-range Coulomb potential and steric effects from the nonzero ion volumes lead to the physical properties that differ greatly from dilute electrolytes. Ionic liquids commonly have large electrochemical windows,3 high thermal stability,<sup>4</sup> and are nonvolatile.<sup>5</sup>

Electrical double-layer supercapacitors store energy in the layer of ions formed at a charged electrode. In ionic liquids, the ions can form multiple layers near a charged surface, in a process that is strongly dependent on the ion concentration and the potential of the charged surface. At a low surface potential, the oppositely charged counterions in the liquid aggregate near the surface and typically overcompensate or *overscreen* the charge in the solid. A second layer composed of co-ions (carrying charge with the same sign as the surface potential) forms to make up for this overcompensation. This process repeats with alternating layers of ions, resulting in a

damped oscillatory charge distribution normal to the interface with a small total charge.

Once the surface potential is large enough that a single layer of counterions is unable to neutralize the electric field, a thicker layer of counterions will form at the electrode, a phenomenon known as *crowding* or *saturation*. Thus, a crowded layer is, by definition, a counterion layer thicker than a monolayer. The structure of these crowded layers depends on the sign of the surface potential due to the asymmetries in size, shape, and surface interactions between the cation and anion. Enhancing the electrolyte properties relevant to energy storage requires a more thorough understanding of how the electrolyte responds to the charged electrode and how the interfacial structures that arise can be controlled and modified.

Recently, mixtures of ionic liquids with molecular solvents have been studied via simulation<sup>9–11</sup> and experiment.<sup>12–18</sup> Adding solvent to the electrolyte mixture can greatly decrease the viscosity of the ionic liquid while increasing both conductivity<sup>14,15</sup> and capacitance.<sup>16,17</sup> A nonmonotonic relationship between capacitance and amount of solvent has

Received: January 5, 2022 Revised: April 27, 2022



been reported for mixtures of solvent and ionic liquid, <sup>15</sup> with a maximum reached at 5–10 mol % ionic liquid. This change in capacitance must be the result of changes in the liquid structure in the vicinity of the electrode. By understanding the solvent effects on the electric double-layer charging process, more dimensions for electrolyte design may be opened up, and the number of applications for ILs may grow. Of specific interest are the effects of solvent concentration and solvent species. (In this work, the word "solvent" refers specifically to any neutral molecular liquid added to an ionic liquid.)

We have previously 19 used X-rays to study the crowded layer that forms within a pure IL at an electrode interface when the applied voltage is high enough (but still within the electrochemical window). We present here an X-ray reflectivity study of crowded layers on an electrode—electrolyte system, using the ionic liquid  $[P_{14,6,6,6}]^+[NTf_2]^-$  diluted with either propylene carbonate (PC), which has a high dielectric constant (64), or dimethyl carbonate (DMC), which has a low dielectric constant (3.2). The effect of ion concentration, working electrode potential, and solvent species on the interfacial ion distribution is explored. Our data indicate that these layers are not pure close-packed counterions and that electrostatic screening by these layers shows an anomalous dependence on the charge density in the layers.

# **■ EXPERIMENTAL SECTION**

The ionic liquid [P<sub>14,6,6,6</sub>]<sup>+</sup>[NTf<sub>2</sub>]<sup>-</sup>, purchased from IoLiTec, was placed in a vacuum oven at 100 °C for 48 h prior to the experiments to remove water and other volatile impurities. The solvents propylene carbonate (PC) and dimethyl carbonate (DMC) were purchased from Sigma-Aldrich in anhydrous form and used as is. The IL/solvent mixtures were injected into a transmission-geometry electrochemical cell (Figure 1a) constructed from Kel-F and sealed against leaks using O-rings and Kapton film windows. To prepare a working electrode that can reflect an X-ray beam, a HF-containing buffered oxide etch (Sigma-Aldrich) was used to remove the oxide layer from a clean 4 × 7 mm silicon wafer with a 3 Å RMS roughness (Ted Pella). (Warning: buffered oxide etch contains hydrofluoric acid; proper protective gear and extreme caution must be used when handling.) The potentials of the Si working electrode and Au wire counter electrode were controlled using a Digi-Ivy DY2311 potentiostat and a Au wire pseudoreference electrode placed in the bulk liquid. Cyclic voltammetry data were collected for each mixture to verify that the electrochemical cell was operating normally (Supporting Informa-

Specular X-ray reflectivity measurements of the Si working electrode-liquid electrolyte interface were conducted at Beamline 33-BM-C of the Advanced Photon Source, Argonne National Laboratory. The incident X-ray beam with an energy of 20 keV and collimated to  $0.5 \text{ mm} \times 0.5 \text{ mm}$  entered the side of the cell through a Kapton window, reflected off the top of the Si working electrode, and was captured by a Pilatus 100 K area detector. After correcting for Xray footprint, sample attenuation, and variable incoming flux and subtracting the simultaneously captured off-specular background, the specular reflectivity data were obtained. Our previous study of the dynamics of crowded layer formation in this IL20 showed that the crowded layer thickness can take several minutes (10<sup>2</sup>-10<sup>3</sup> s) to stabilize. Therefore, after any change in the voltage, the system was allowed to equilibrate for 20 min before X-ray reflectivity measurements of the Si-liquid interface were performed. Each measurement was repeated at least 3 times to confirm that the reflectivity is constant in time and that no X-ray damage had taken place.

By measuring reflectivity R as a function of the momentum transfer in the direction normal to the interface  $q_z = 2k_z \sin \theta$ , the electron density profile near the interface can be determined. It can be shown<sup>21</sup> that the reflectivity  $R(q_z)$  is given by

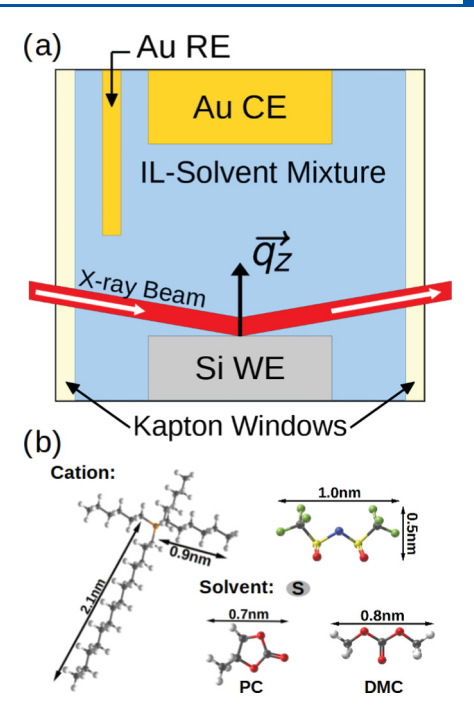


Figure 1. (a) Schematic diagram of the 20x6x6mm electrochemical cell. The ionic liquid/solvent mixture is injected into the cell containing a polished silicon working electrode (WE), a gold wire counter electrode (CE), and a gold wire pseudoreference electrode (RE), all connected to a potentiostat. The incident X-rays are reflected off the silicon WE and collected by an area detector. (b) The chemical species present in the cell are trihexyltetradecylphosphonium (P<sub>14,6,6,6</sub>) cations, bis(trifluoromethylsulfonyl)imide (NTf<sub>2</sub>) anions, and propylene carbonate (PC) or dimethyl carbonate (DMC) as a solvent. Element-color keys: H (white), C (gray), N (blue), O (red), F (green), P (orange), and S (yellow).

$$\frac{R(q_z)}{R_F(q_z)} = \left| \int_{-\infty}^{\infty} \frac{\partial \rho(z)}{\partial z} e^{iq_z z} dz \right|^2$$
 (1)

where  $R_{\rm F}$   $(q_z)$  is the Fresnel reflectivity from an ideal, infinitely sharp interface. The ratio depends on the variation of the electron density  $\rho(z)$  across the interface. Reflectivity data  $R_{\rm obs}$  are fitted as follows: choose a model for  $\rho(z)$ , calculate the reflectivity R for an initial guess of  $\rho(z)$ , and then refine the guess by attempting to minimize  $\sum (\log R_{\rm obs} - \log R)^2$ . (Fitting the logarithm of R reduces overfitting of the low-q data, which is several orders of magnitude greater in value than data at the highest values of q.) We were unable to fit our reflectivity data when modeling the electron density profile as a monotonic or oscillating exponential decay, as in ref 18. However, the data could be fitted satisfactorily with a "slab model": the liquid nearest the surface is described by one or two interfacial slabs of constant electron density  $\rho_v$  finite thickness  $D_v$  and roughness  $\sigma_i$  located at position  $h_i$  enclosed by semi-infinite slabs for the electrode and bulk liquid

$$\rho(z) = \rho_0 + \sum_{i=0}^n \frac{\rho_{i+1} - \rho_i}{2} \left[ 1 + \text{erf}\left(\frac{z - h_i}{\sqrt{2}\sigma_i}\right) \right] \quad h_j = \sum_{i=0}^j D_j$$
(2)

The parameters characterizing the slabs  $(D_i, \rho_i)$  and  $\sigma_i$ ) were refined via a genetic fitting algorithm using the IGOR package Motofit.<sup>23</sup>

The effect of applied potential and RTIL fraction of the mixture on the thickness and density of the interfacial layer is the focus of this work. A one-slab model was used whenever it is sufficient to fit the data. When the one-slab model could not capture the reflectivity data features adequately, a two-slab model was used. This can occur when the first minimum approaches low- $q_z$  values ( $q_z < 0.1 \text{ Å}^{-1}$ ) and the

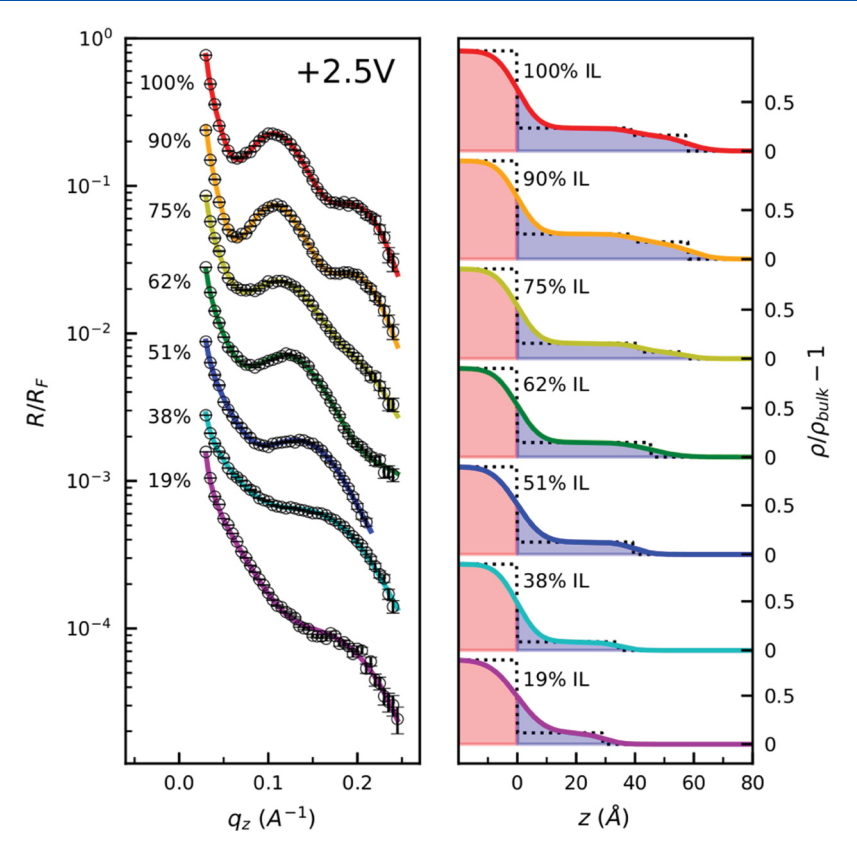


Figure 2. (Left) Normalized reflectivity data for mixtures of propylene carbonate and ionic liquid near a charged silicon electrode. Data from different mixtures (labeled by the volume percentage of IL) are offset vertically with respect to each other for clarity. (Right) Electron density profiles obtained from fitting reflectivity data with the slab model (solid lines). The same profiles with interface roughness set to zero are shown with dashed lines, and these clearly show the interfacial "slabs" (crowded layers).

interfacial region becomes too large to accurately describe with a single constant electron density. In these cases, the total sum of the thicknesses  $D=D_1+D_2$  and the thickness-weighted average of the electron densities  $\rho=(D_1\rho_1+D_2\rho_2)/(D_1+D_2)$  are reported, rather than individual values, to enable comparisons to the one-slab fits. A detailed list of best-fit parameters is given in the Supporting Information.

X-ray reflectivity with a monochromatic beam is not sensitive to different elements but "sees" only electron densities. The chemical structures of the liquids used are shown in Figure 1b. Volumes and electron densities of the anions, cations, and solvents used are listed in the Supporting Information. The  $[P_{14,6,6,6}]^+$  cations are relatively large  $(\sim\!0.95~\text{nm}^3)$  and their electron density (289 electrons/nm³) is only slightly less than that of the bulk liquid (347 electrons/nm³). The NTf $_2^-$  anions are small  $(\sim\!0.24~\text{nm}^3)$  and have a significantly higher electron density (577 electrons/nm³). Thus, an observed change in the electron density at the interface relative to the bulk liquid can be interpreted as a change in the molecular composition in that region.

Since the interfacial layers we observe as functions of applied voltage are reversible and reproducible, we attribute them to an imbalance in cations and anions, resulting from counterions attracted to the electrode surface and co-ions repelled. The average charge density  $\rho_e$  within an interfacial slab of the electron number density  $\rho_I$  can then be calculated using 19

$$\rho_{Q} = Q(\rho_{I} - \rho_{B}) \frac{V_{A} + V_{C}}{V_{A}N_{C} - V_{C}N_{A}}$$
(3)

where Q is the charge carried by the counterion (-e in the case of a monovalent IL at a positive electrode),  $\rho_{\rm I}$  and  $\rho_{\rm B}$  are the electron densities at the interface and bulk liquid, respectively,  $V_{\rm A}/V_{\rm c}$  are the volumes of the anion/cation, and  $N_{\rm A}/N_{\rm c}$  are the numbers of electrons carried by the anion/cation. For a proof of the above equation, which applies to pure ILs, see the Supporting Information. The quantity

 $\rho_{\rm I}$ – $\rho_{\rm B}$  will be referred to in the rest of this paper as the excess electron density of the interfacial layer. Since the fitting of reflectivity also gives us the slab thickness  $D_{\rm r}$ , the surface charge density (charge per unit area)  $\sigma_{\rm O}=\rho_{\rm O}\,D$  can be calculated.

In an ionic liquid—solvent mixture, a difference in the concentration of solvent in the bulk liquid and the interfacial layer also causes a difference in electron density but one that does not contribute to the surface charge. In general, it is not possible to determine the proportions within the layer of three species of different electron densities (cation, anion, and solvent) using a single measurement of the excess electron density of the interfacial layer. However, if the average solvent concentration in the interfacial layer is the same as in the bulk solvent (as discussed later in this paper), the charge density can once again be calculated without ambiguity

$$\rho_{Q} = Q(\rho_{I} - \rho_{B}) \frac{(1 - x_{S}^{B})(V_{C} + V_{A}) + x_{S}^{B} 2V_{S}}{(1 - x_{S}^{B})\alpha_{CA} + x_{S}^{B}(\alpha_{CS} - \alpha_{AS})}$$
(4)

where  $\alpha_{ij} = N_i \ V_j - N_j \ V_i$  and  $\alpha_S^S$  is the number fraction of solvent molecules in the mixture. This equation is also proved in the Supporting Information.

# ■ RESULTS AND DISCUSSION

In all IL/solvent mixtures of any IL vol %, our reflectivity data contain no interference features in the range  $q_z < 0.3~\text{Å}^{-1}$  until a threshold voltage is reached, around 1.6-1.8~V. In other words, within the spatial resolution of the experiment ( $\Delta z = \pi/q_{\text{max}} \approx 11~\text{Å}$ ), there is no significant contrast in electron density between the liquid near the electrode surface and far away from it. If there are surface effects such as alternating layers of anions and cations (overscreening) at the lower voltages, the

density variations are too small to affect the reflectivity signal in the range we observe.

At working electrode voltages higher than 1.6 V, minima in the reflectivity curve appear (Figure 2). They indicate that in addition to the electrode surface, there is at least one additional interface where the electron density changes sharply—the minima are due to interference between reflections at these two interfaces. We reemphasize that we cannot fit the reflectivity minima by assuming monotonically decaying or oscillating-decaying electron density profiles. The success of the slab model in fitting the data signals the formation of a crowded layer at the electrode.

Reflectivity curves of different mixtures held at the same voltage (Figure 2, left) feature one or more minima that move toward  $q_z=0$  in mixtures of higher IL concentrations. This corresponds to an increasing electron-dense layer thickness (Figure 2, right) as the bulk IL concentration increases, and this trend will be discussed below. In the voltage range studied, the layer is 1.5-2 times as thick in pure IL than in 19 vol % IL (the most dilute case for which reflectivity features were observed).

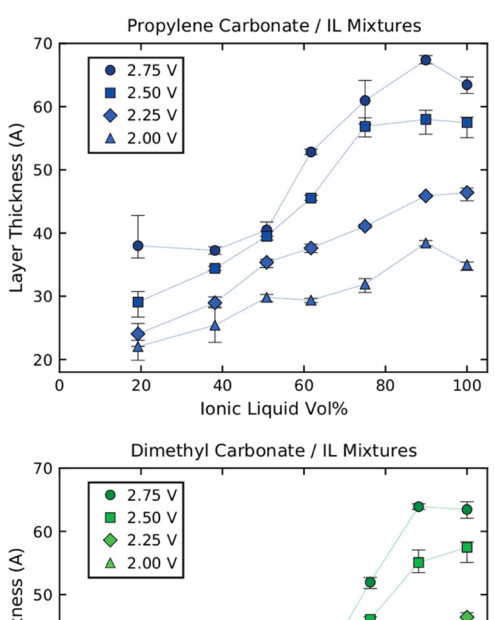
A reflectivity study of IL-containing mixtures near charged sapphire observed a similar increase in the thickness of the interfacial layer region, which was attributed to the bulk screening length increasing with more ions present, reducing the exponential damping of the alternating ion layers. However, that study was of alternating cation and anion layers at low voltages (overscreening), while the present study is of crowded layers at higher voltages. Thus, the two experiments are not directly comparable, although the trend is qualitatively the same.

The layer thickness for all mixtures increases when the voltage is increased. Figure 3 shows the layer thickness as a function of IL vol % for mixtures of solvent and IL at different voltages.

The mass density of each solution was measured via gravimetric analysis and used to calculate the bulk electron density  $\rho_{\rm B}$  of each mixture. The excess electron density in the interfacial layer was calculated by subtracting  $\rho_{\rm B}$  from the slab electron density  $\rho_{\rm I}$  (determined from fitting reflectivity data). In Figure 4, the excess density is shown for pure IL (black), PC/IL solutions (blue), and DMC/IL solutions (green). We found no clear dependence of the excess density on voltage in the range of 2.00–2.75 V; thus, the mean excess density value from four data sets at voltages between 2.00 and 2.75 V is reported, and the standard deviation is indicated by the error bars.

In pure  $[P_{14,6,6,6}][NTf_2]$ , the smaller anions take up only 20% of the volume  $(V_A = 0.239 \text{ nm}^3, V_C = 0.946 \text{ nm}^3)$ . The electron densities of the cation, anion, and bulk IL are 289, 577, and 347 electrons/nm³ respectively. (Electron density, molecule/ion volume, and other information on the materials used are tabulated in the Supporting Information.) At electrode voltages positive enough to form a crowded layer of anions, the interfacial electron density obtained from the slab model for the pure IL is 419  $\pm$  5 electrons/nm³, which is less than the density of the anion (see above). From this, we calculate, using eq 3, that the number ratio of anions to cations in the crowded layer formed from the pure IL is 3.3  $\pm$  0.2. (These data are consistent with those in a previous study<sup>19</sup> by our group on the same IL.)

Reflectivity data for IL solutions, i.e., IL mixed with propylene carbonate (Figure 2) or with dimethyl carbonate,



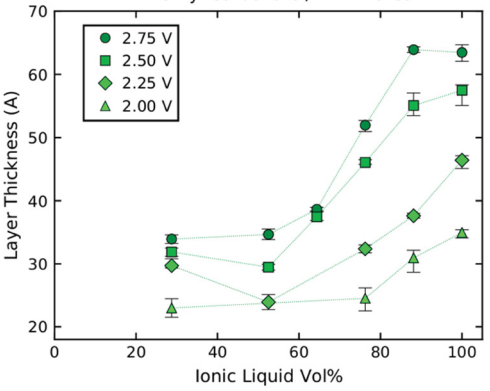


**Figure 3.** Thickness of the interfacial layer near the charged electrode for mixtures of PC/IL (top) and DMC/IL (bottom) obtained from fitting X-ray reflectivity data to a slab model. Dotted lines are guides to the eye.

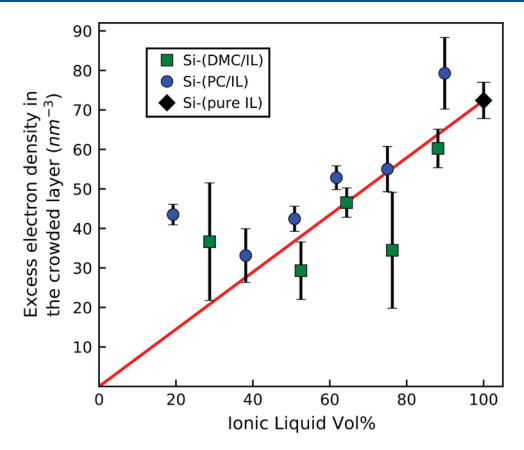


**Figure 4.** Amount by which the electron density of the crowded interfacial layer exceeds that of the bulk solution (i.e.,  $\rho_{\rm I}-\rho_{\rm B}$ ), as a function of the IL concentration (vol %) in the bulk solution. Since the interfacial density shows no clear voltage dependence, the data have been averaged over different voltages of 2.00–2.75 V at each solution concentration. The red line is not a fit to the data but linearly connects the excess electron density of the pure IL sample with the origin. Scaling of the excess interfacial density with the bulk IL concentration implies that the crowded layer contains the same fraction of solvent as the bulk IL.

also indicate the formation of a crowded layer of anions after approximately the same threshold voltage of  $\sim 1.7~V$  is reached. The bulk electron density increases when adding PC (which is slightly more electron-dense at 383 electrons/nm³) and stays

almost constant when adding DMC (343 electrons/nm³). The electron density in the crowded layer is greater in all samples than that of the bulk IL solution, indicating that there are more anions than cations, but it is always lower than the density of an anion-only layer, indicating that other less electron-dense species, cations and solvent, are present. (Detailed X-ray reflectivity fitting data are given in the Supporting Information.)

As the ionic liquid fraction in the mixture decreases, the excess densities of the crowded layer roughly follow a line connecting the pure IL data point with the origin (Figure 4, red line). At lower concentrations (<50 vol % IL), there may be a small deviation from this trend (Figure 4), but since it occurs where the excess density and layer thicknesses are quite small, we cannot tell whether this trend is significant. Using the excess density data for mixtures >50 vol % IL, we estimate the anion:cation ratio in the crowded layer to be 4.6  $\pm$  0.6 for IL/PC and 3.2  $\pm$  0.8 for IL/DMC.

Figure 4 explicitly contradicts a simple picture of a crowded layer as a "pile-up" of counterions (and only counterions) attracted to the electrode surface, so that the density is determined solely by steric repulsion of a pure layer of anions. If that were the case, the interfacial density would be independent of the bulk solution concentration. Theories describing the crowded layer structure that utilize this assumption<sup>24</sup> may need to be revisited. In reality, the crowded layer excess density scales linearly with bulk concentration (Figure 4), which suggests that the solvent concentration in the crowded layer is about the same (within roughly  $\pm 10\%$ ) as in the bulk. The cation:ion ratio would then be the same as in the pure liquid, but the excess density is reduced, as seen in Figure 4, simply because of solvent dilution. This means that the crowded layers, while thicker than a monolayer and therefore consistent with the definition of crowding, are not always packed with a density determined by ion sizes (steric repulsion). The trend seen in Figure 4 justifies our use of eq 4, which assumes a constant solvent density.

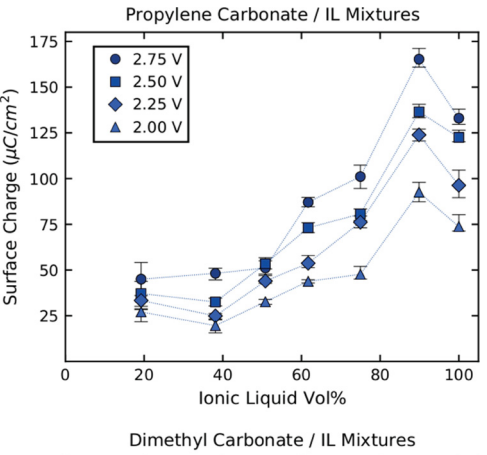
One might expect that the electrostatic attraction of anions to the electrode will tend to exclude the solvent molecules in the crowded layer. However, our result simply means that the solvents "dissolve" the crowded layer just as they dissolve the bulk IL. The chemical potential of the solvent, which is a function of solvent concentration, must be the same on both sides of the crowded layer-bulk IL interface, and thus a significant concentration gradient is unlikely. If any solvent concentration gradient exists in our systems, it is small (within the  $\pm 10\%$  range of our data). Indeed, a simulation by Zhang et al. 25 also showed the presence of solvent in the IL layer immediately next to a positive graphite electrode. Recent neutron reflectivity measurements by Pilkington et al. 26 of IL/ PC mixtures near a Au electrode also support the idea of solvent remaining in the crowded layer at both positive and negative electrode voltages.

One could alternatively propose that the solvent does not penetrate (or only partially penetrates) the crowded layer, but for some reason, the anion/cation ratio in the crowded layer also varies, in such a way as to mimic the effect of roughly equal solvent densities in the interface layer and the bulk (Figure 4). Even apart from the gradient in solvent chemical potential that would be introduced, we know of no good reason for such a coincidence. Further, such a phenomenon would also lead to the same qualitative trend: the charge densities in the crowded layer will decrease as the bulk solution

becomes more dilute. Thus, the qualitative conclusions of this paper would remain unchanged.

The total surface charge per unit area  $\sigma$  can be calculated using eq 4 and the layer thickness D obtained from the reflectivity data. When solvent is added, we observe a general trend of the thickness D and excess electron density  $\rho_{\rm I}$ – $\rho_{\rm B}$  decreasing (Figures 3 and 4). These two effects combined reduce the total surface charge of the crowded layer in solutions with lower IL content.

For PC/IL mixtures (Figure 5, top), at all voltages, the surface charge reaches a maximum at 89 vol % IL before



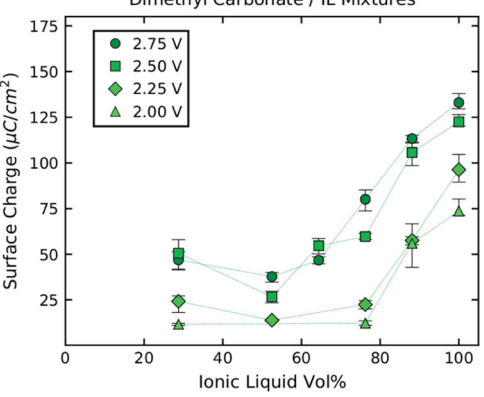


**Figure 5.** Magnitude of the surface charge per unit area of the interfacial layer for mixtures of PC/IL (top) and DMC/IL (bottom). These data are derived from those in Figures 3 and 4. Dotted lines connecting the points are guides to the eye.

decreasing at other amounts of IL. By examining Figures 3 and 4, it can be seen that this is due to this mixture having a higher excess electron density (due to anions) in the layer compared to pure IL while still maintaining a similar layer thickness. The DMC/IL mixtures (Figure 5, bottom) do not have such a maximum, and generally surface charge increases as IL concentration increases.

There are many measurements of capacitance in such IL–electrode systems, but capacitance can mean different things in different contexts. Our X-ray determinations of surface charge allow us to calculate the d.c. total capacitance Q/V (the property relevant to long-term energy storage). On the other hand, laboratory capacitance measurements are usually of the differential capacitance dQ/dV at some voltage offset, measured using a.c. signals. Such measurements depend on the voltage offset because Q is not a linear function of V and also on the frequency because of the various IL time scales.  $^{8,20}$ 

Nonetheless, a comparison with a.c. capacitance measurements in IL solutions is suggestive. The mixture of PC/IL with the highest IL composition (89 vol % IL) we studied was found to have the higher density layer, resulting in a maximum in surface charge and thus in d.c. capacitance. A nonmonotonic dependence on IL concentration has been observed for several characteristics of solvent/IL mixtures, including conductivity<sup>14</sup> and a.c. capacitance. 15 The capacitance maximum in PC/IL mixtures found in the latter study by Bozym et al. 15 via electrochemical impedance spectroscopy was found to be at 35 vol % IL. However, when accounting for the larger size of the cation in the IL in our system compared to that used in their study, the resulting absolute bulk concentration of the ions becomes similar (1.35 M in ref 15, 1.26 M in this work). This indicates that a possible capacitance maximum can be predicted based on the ion concentration rather than the IL volume fraction of the mixture. Note, however, that no such maximum is seen in DMC-IL mixtures.

Our data contain several unexpected features. First, as previously noted, our data are consistent with the solvent fraction being roughly the same in the crowded layer as in the bulk mixture. Second, the crowded layer near the positive electrode, while naturally anion-rich, is never pure anions; there is always a significant fraction of cations. As previously discussed, this follows from the experimental finding that the crowded layer density is higher than the bulk density but lower than the density of a pure anion layer. This was previously found in the pure  ${\rm IL}^{19,20}$  but it is true also true for  ${\rm IL}$ —solvent mixtures. Certainly, entropy considerations imply that at nonzero temperature one can never have a region composed purely of anions even if that is the lowest-electrostatic-energy state. However, we do not have a quantitative explanation for the large fraction of cations seen. It is possible that a statistical model would make predictions that can be compared to our results, but we are not aware of such a model in the existing literature.

Third and most important, at a given voltage, both the thickness and density of the crowded layer (and thus the surface charge) decrease when the solution becomes more dilute (the IL concentration decreases). The crowded layer thickness is a measure of the distance in which the electric field decays to a value below the threshold for further crowding. This trend is anomalous because the charge density in the crowded layer decreases as the solution becomes more dilute, and so one expects that the electric field would penetrate further into the fluid. To make this quantitative, one can use Gauss' law of electrostatics to calculate the voltage across a layer of uniform charge density  $\rho_O$  and thickness D next to a conducting electrode carrying the opposite charge. Assuming that the electric field on the far side, i.e., at the interface with the bulk liquid, is negligible, one readily obtains  $V = \rho_0 D^2 / 2\varepsilon$ . Thus, for the same applied voltage, a decrease in  $\rho_0$  requires an increase in D. (We do not see crowded layers until the voltage is above ~1.7 V, which suggests that the electric field at the crowded layer-bulk liquid interface is nonzero. This does not change the qualitative prediction that a slab with a smaller charge density needs to be thicker, which is the opposite of what we see.)

Another way to state the problem is to look at the trend in DC capacitance shown in Figure 5. Such trends are also seen in AC capacitance, but in those studies, nanoscale information is not available, and the behavior can potentially be explained in terms of the dynamic response of the ions. The DC trend is

much harder to explain because here we also know the static nanoscale structure! At a given voltage, a thinner capacitor holds more charge, i.e., the capacitance per unit area is higher. (This is a consequence of Gauss' law.) However, in our case, we see the opposite: the surface charge at a given voltage is smaller in the more dilute samples (Figure 5), even though that is when the average distance between these charges and the electrode surface is smaller (Figure 3).

Our results may appear similar to recent studies  $^{27-30}$  showing that the electrostatic screening length in bulk ionic solutions increases with increasing ion concentration at high concentrations. This is the opposite of what is seen at lower concentrations (and what is predicted by the Debye–Hückel theory), but the qualitative trend is also seen in simulations and theories.  $^{32-34}$  One likely explanation for this behavior is increased correlations at high concentrations, in contrast to the Debye picture where the ions move independently. Certainly, our liquids also have high ion densities, but that is where the similarities end. The crowded layer is not an equal mixture of anions and cations; even if the  $\sim 23\%$  of cations is highly correlated with the corresponding fraction of anions, there are enough unpaired anions left over for the layer to be analyzed using our Gauss's law arguments.

Of course, there are many ways in which our simple electrostatics analysis could fail and indeed must fail. One possibility is that the dielectric constant might be very different from that in the bulk, and a strong function of the bulk solution concentration. We know of no simple reason why this should be so. The bulk dielectric constants  $\varepsilon$  of the liquids used are tabulated in the Supporting Information. It can be seen that PC has 20 times the dielectric constant of DMC, yet the layer thickness and surface charge are very similar to the two solvents at any given voltage and IL concentration. Of course, at the nanoscale, bulk dielectric constants are not necessarily meaningful quantities, and the effective  $\varepsilon_r$  is not simply a weighted average of the bulk values of the constituents. Interactions between the anions, cations, and solvents, and the resulting structural effects, could cause the electrostatic response of this 2-7 nm region to be quite different from those of any of the bulk constituents.

Further, it is not necessarily true that each IL anion carries charge  $\pm e$ . Kjellander and co-workers  $^{35-37}$  have developed theories relevant to ionic liquids that involve "dressed" ions with renormalized charge, and these theories also result in a renormalized dielectric permittivity. It remains to be seen whether these or similar approaches can be applied to the charged, crowded layers we have studied and whether this will lead to a better understanding of the anomalous trends reported here.

## CONCLUSIONS

Dense "crowded" layers composed primarily but not purely of anions, next to positive electrodes, extend further into the bulk liquid than less dense layers at the same applied voltage. This means that less densely charged layers cause the electrostatic field to decay over shorter distances than more densely charged layers do. This counterintuitive trend is reminiscent of that reported in bulk ionic solutions but occurs under very different conditions.

# ASSOCIATED CONTENT

# Supporting Information

The Supporting Information is available free of charge at https://pubs.acs.org/doi/10.1021/acs.langmuir.2c00036.

Mol percentage vs volume percentage; calculating the charge density of mixtures; table of electron densities; cyclic voltammetry data; and table of best-fit parameters (PDF)

## AUTHOR INFORMATION

#### **Corresponding Author**

Pulak Dutta — Department of Physics & Astronomy, Northwestern University, Evanston, Illinois 60208, United States; orcid.org/0000-0002-2111-0546; Email: pdutta@northwestern.edu

#### **Authors**

Travis Douglas – Department of Physics & Astronomy, Northwestern University, Evanston, Illinois 60208, United States; orcid.org/0000-0002-0817-7674

Sangjun Yoo — Department of Physics & Astronomy, Northwestern University, Evanston, Illinois 60208, United States; © orcid.org/0000-0003-0525-204X

Complete contact information is available at: https://pubs.acs.org/10.1021/acs.langmuir.2c00036

#### Notes

The authors declare no competing financial interest.

## ACKNOWLEDGMENTS

This work was supported by the U.S. National Science Foundation under award no. 1665255. This research used resources of the Advanced Photon Source, a U.S. Department of Energy (DOE) Office of Science User Facility operated for the DOE Office of Science by Argonne National Laboratory under Contract No. DE-AC02-06CH11357. The authors thank Jenia Karapetrova (APS 33-BM) for her assistance during experiments and Susan Perkin and Roland Kjellander for their helpful discussions.

# REFERENCES

- (1) Zhong, C.; Deng, Y.; Hu, W.; Qiao, J.; Zhang, L.; Zhang, J. A Review of Electrolyte Materials and Compositions for Electrochemical Supercapacitors. *Chem. Soc. Rev.* **2015**, *44*, 7484–7539.
- (2) Fedorov, M. V.; Kornyshev, A. A. Ionic Liquids at Electrified Interfaces. *Chem. Rev.* **2014**, *114*, 2978–3036.
- (3) Matsumoto, K.; Hagiwara, R.; Ito, Y. Room-Temperature Ionic Liquids with High Conductivities and Wide Electrochemical Windows. *Electrochem. Solid-State Lett.* **2004**, *7*, No. E41.
- (4) Paulechka, Y. U.; Zaitsau, D. H.; Kabo, G. J.; Strechan, A. A. Vapor Pressure and Thermal Stability of Ionic Liquid 1-Butyl-3-Methylimidazolium Bis(Trifluoromethylsulfonyl)Amide. *Thermochim. Acta* 2005, 439, 158–160.
- (5) Ionic Liquids in Synthesis, Wasserscheid, P.; Welton, T., Eds.; Wiley-VCH Verlag: Weinheim, Germany, 2015.
- (6) Kornyshev, A. A. Double-Layer in Ionic Liquids: Paradigm Change? J. Phys. Chem. B 2007, 111, 5545-5557.
- (7) Bazant, M. Z.; Storey, B. D.; Kornyshev, A. A. Double Layer in Ionic Liquids: Overscreening versus Crowding. *Phys. Rev. Lett.* **2011**, *106*, No. 046102.
- (8) Uysal, A.; Zhou, H.; Feng, G.; Lee, S. S.; Li, S.; Cummings, P. T.; Fulvio, P. F.; Dai, S.; McDonough, J. K.; Gogotsi, Y.; Fenter, P. Interfacial Ionic "Liquids": Connecting Static and Dynamic Structures. *J. Phys. Condens. Matter* **2015**, 27, No. 032101.

- (9) Borodin, O.; Henderson, W. A.; Fox, E. T.; Berman, M.; Gobet, M.; Greenbaum, S. Influence of Solvent on Ion Aggregation and Transport in PY15TFSI Ionic Liquid-Aprotic Solvent Mixtures. *J. Phys. Chem. B* **2013**, *117*, 10581–10588.
- (10) Feng, G.; Huang, J.; Sumpter, B. G.; Meunier, V.; Qiao, R. Structure and Dynamics of Electrical Double Layers in Organic Electrolytes. *Phys. Chem. Chem. Phys.* **2010**, *12*, 5468–5479.
- (11) Vatamanu, J.; Vatamanu, M.; Borodin, O.; Bedrov, D. A Comparative Study of Room Temperature Ionic Liquids and Their Organic Solvent Mixtures near Charged Electrodes. *J. Phys. Condens. Matter* **2016**, 28, No. 464002.
- (12) Couadou, E.; Jacquemin, J.; Galiano, H.; Hardacre, C.; Anouti, M. A Comparative Study on the Thermophysical Properties for Two Bis[(Trifluoromethyl)Sulfonyl]Imide-Based Ionic Liquids Containing the Trimethyl-Sulfonium or the Trimethyl-Ammonium Cation in Molecular Solvents. J. Phys. Chem. B 2013, 117, 1389—1402.
- (13) Jan, R.; Rather, G. M.; Bhat, M. A. Effect of Cosolvent on Bulk and Interfacial Characteristics of Imidazolium Based Room Temperature Ionic Liquids: Impact of Cosolvent on Physciochemical Characteristics of Ionic Liquids. *J. Solution Chem.* **2014**, *43*, 685–695.
- (14) Ruiz, V.; Huynh, T.; Sivakkumar, S. R.; Pandolfo, A. G. Ionic Liquid—Solvent Mixtures as Supercapacitor Electrolytes for Extreme Temperature Operation. *RSC Adv.* **2012**, *2*, 5591—5598.
- (15) Bozym, D. J.; Uralcan, B.; Limmer, D. T.; Pope, M. A.; Szamreta, N. J.; Debenedetti, P. G.; Aksay, I. A. Anomalous Capacitance Maximum of the Glassy Carbon-Ionic Liquid Interface through Dilution with Organic Solvents. *J. Phys. Chem. Lett.* **2015**, *6*, 2644–2648.
- (16) Zhang, Q.; Liu, X.; Yin, L.; Chen, P.; Wang, Y.; Yan, T. Electrochemical Impedance Spectroscopy on the Capacitance of Ionic Liquid—Acetonitrile Electrolytes. *Electrochim. Acta* **2018**, 270, 352—362.
- (17) Gu, C.; Yin, L.; Li, S.; Zhang, B.; Liu, X.; Yan, T. Differential Capacitance of Ionic Liquid and Mixture with Organic Solvent. *Electrochim. Acta* **2021**, *367*, No. 137517.
- (18) Mezger, M.; Roth, R.; Schröder, H.; Reichert, P.; Pontoni, D.; Reichert, H. Solid-Liquid Interfaces of Ionic Liquid Solutions–Interfacial Layering and Bulk Correlations. *J. Chem. Phys.* **2015**, *142*, No. 164707.
- (19) Chu, M.; Miller, M.; Dutta, P. Crowding and Anomalous Capacitance at an Electrode-Ionic Liquid Interface Observed Using Operando X-Ray Scattering. ACS Cent. Sci. 2016, 2, 175–180.
- (20) Chu, M.; Miller, M.; Douglas, T.; Dutta, P. Ultraslow Dynamics at a Charged Silicon—Ionic Liquid Interface Revealed by X-Ray Reflectivity. *J. Phys. Chem. C* **2017**, *121*, 3841—3845.
- (21) Als-Nielsen, J.; McMorrow, D. Elements of Modern X-Ray Physics: Als-Nielsen/Elements, 2nd ed.; Wiley-Blackwell: Hoboken, NJ, 2011
- (22) Parratt, L. G. Surface Studies of Solids by Total Reflection of X-Rays. *Phys. Rev.* **1954**, *95*, 359–369.
- (23) Nelson, A. Co-Refinement of Multiple-Contrast Neutron/X-Ray Reflectivity Data UsingMOTOFIT. *J. Appl. Crystallogr.* **2006**, 39, 273–276.
- (24) Kilic, M. S.; Bazant, M. Z.; Ajdari, A. Steric Effects in the Dynamics of Electrolytes at Large Applied Voltages. I. Double-Layer Charging. *Phys. Rev. E* **2007**, *75*, No. 021502.
- (25) Zhang, S.; Bo, Z.; Yang, H.; Yang, J.; Duan, L.; Yan, J.; Cen, K. Insights into the Effects of Solvent Properties in Graphene Based Electric Double-Layer Capacitors with Organic Electrolytes. *J. Power Sources* **2016**, 334, 162–169.
- (26) Pilkington, G. A.; Oleshkevych, A.; Pedraz, P.; Watanabe, S.; Radiom, M.; Reddy, A. B.; Vorobiev, A.; Glavatskih, S.; Rutland, M. W. Electroresponsive Structuring and Friction of a Non-Halogenated Ionic Liquid in a Polar Solvent: Effect of Concentration. *Phys. Chem. Chem. Phys.* **2020**, 22, 19162–19171.
- (27) Gebbie, M. A.; Valtiner, M.; Banquy, X.; Fox, E. T.; Henderson, W. A.; Israelachvili, J. N. Ionic Liquids Behave as Dilute Electrolyte Solutions. *Proc. Natl. Acad. Sci. U. S. A.* **2013**, *110*, 9674–9679.

- (28) Smith, A. M.; Lee, A. A.; Perkin, S. The Electrostatic Screening Length in Concentrated Electrolytes Increases with Concentration. *J. Phys. Chem. Lett.* **2016**, *7*, 2157–2163.
- (29) Lee, A. A.; Perez-Martinez, C. S.; Smith, A. M.; Perkin, S. Underscreening in Concentrated Electrolytes. *Faraday Discuss.* **2017**, 199, 239–259.
- (30) Coles, S. W.; Smith, A. M.; Fedorov, M. V.; Hausen, F.; Perkin, S. Interfacial Structure and Structural Forces in Mixtures of Ionic Liquid with a Polar Solvent. *Faraday Discuss.* **2018**, 206, 427–442.
- (31) Coles, S. W.; Park, C.; Nikam, R.; Kanduč, M.; Dzubiella, J.; Rotenberg, B. Correlation Length in Concentrated Electrolytes: Insights from All-Atom Molecular Dynamics Simulations. *J. Phys. Chem. B* **2020**, *124*, 1778–1786.
- (32) Lee, A. A.; Perez-Martinez, C. S.; Smith, A. M.; Perkin, S. Scaling Analysis of the Screening Length in Concentrated Electrolytes. *Phys. Rev. Lett.* **2017**, *119*, No. 026002.
- (33) Coupette, F.; Lee, A. A.; Härtel, A. Screening Lengths in Ionic Fluids. *Phys. Rev. Lett.* **2018**, *121*, No. 075501.
- (34) Adar, R. M.; Safran, S. A.; Diamant, H.; Andelman, D. Screening Length for Finite-Size Ions in Concentrated Electrolytes. *Phys. Rev. E.* **2019**, *100*, No. 042615.
- (35) Kjellander, R. Focus Article: Oscillatory and Long-Range Monotonic Exponential Decays of Electrostatic Interactions in Ionic Liquids and Other Electrolytes: The Significance of Dielectric Permittivity and Renormalized Charges. *J. Chem. Phys.* **2018**, *148*, No. 193701.
- (36) Forsberg, B.; Ulander, J.; Kjellander, R. Dressed Ion Theory of Size-Asymmetric Electrolytes: Effective Ionic Charges and the Decay Length of Screened Coulomb Potential and Pair Correlations. *J. Chem. Phys.* **2005**, *122*, No. 064502.
- (37) Kjellander, R. Nonlocal Electrostatics in Ionic Liquids: The Key to an Understanding of the Screening Decay Length and Screened Interactions. *J. Chem. Phys.* **2016**, *145*, No. 124503.

